Generation of Tyro3 Receptor Tyrosine Kinase Clones to Study Interactions with SH2 Domain Proteins in the Retinal Pigment Epithelium

Lauren Harris

Shameka Shelby, Ph.D.

Florida Southern College

Abstract

The retina is comprised of cone and rod photoreceptors that must continually be maintained in order to preserve visual acuity. Daily light exposure to the outer portions of the photoreceptors, termed outer segments (OS), leads to photo-oxidative stress. To combat potential retinal damage caused by light exposure, the Retinal Pigment Epithelium (RPE) phagocytizes spent outer segments. Disruption of OS phagocytosis leads to the accumulation of debris that blocks the flow of oxygen and nutrients to the retina. This will eventually lead to atrophy of the retina and, ultimately, blindness. Previous studies have demonstrated the requirement of Mer Receptor Tyrosine Kinase (MERTK) in the process of OS phagocytosis. Protein interactions between MERTK and SH2 domain proteins Grb2, P85α, Src, and Vav3 have also been shown to be necessary for OS phagocytosis. Recent studies suggest that TYRO3, a familial receptor tyrosine kinase to MERTK, can compensate in the absence of MERTK. As such, I hypothesized that TYRO3 may bind to SH2 domain proteins known to bind to MERTK. To test the similarities of interactions between MERTK, TYRO3, and associated SH2 domain proteins (Grb2, P85α, Src, Vav1, Vav2, and Vav3), various clones of TYRO3 were generated. Two truncated TYRO3 proteins that included the kinase domain and cytoplasmic tail (residues 470 – 890 and 498 – 890) were successfully cloned into a pRSET vector and recombinantly overexpressed. These clones were then purified and potential interactions between the purified Tyro3 and the SH2 domain proteins, which were generously provided by Dr. Shameka Shelby, were assessed using Ni-NTA pulldown assays; however, future pulldowns will need to be conducted to obtain conclusive results. Additionally, full length TYRO3 was successfully cloned into pcDNA3.1 His vector for overexpression in mammalian cultured cells. Further experiments will

confirm the identified interactions in-vitro and will be conducted in mammalian cells transfected with TYRO3. This study has generated the tools necessary to further identify components of the RPE phagocytic mechanism. Elucidation of this mechanism will be instrumental in identifying future retinal disease genes and understanding the impact on proteins that may be involved in Age-related Macular Degeneration.

Introduction

The retina:

The retina is a complex central nervous system (CNS) tissue that is comprised of many components that are essential to vision. This structure is approximately 0.5 mm thick and contains photo-sensing cells – the cone and rod photoreceptors – located towards the more posterior portion of the retina and adjacent to the retinal pigment epithelium (RPE). While the photoreceptors and RPE are the main concern of this study, there are several more important levels of this tissue that light must travel through before the photons are taken in by the photoreceptors, translated into a biochemical message, and then converted to an electrical signal that is subsequently sent to the brain through the optic nerve [1-3].

Anterior to posterior, the layers of the retina are organized as follows: the ganglion cell layer (GCL), inner plexiform layer (IPL), inner nuclear layer (INL), outer plexiform layer (OPL), outer nuclear layer (ONL), photoreceptor inner segments (IS), photoreceptor outer segments (OS), and the retinal pigment epithelium. These layers are arranged so that light passes through the anterior portion of the retina and is received by the posteriorly located photoreceptors. Photons react with the cone and rod photoreceptors, which results in an electrical signal that is transmitted posteriorly to anteriorly through the cell bodies and axons located in the layers of the retina. Axons of the ganglion cell layer then converge to form the optic nerve, which is connected to the brain, which is responsible for visual perception [1-3].

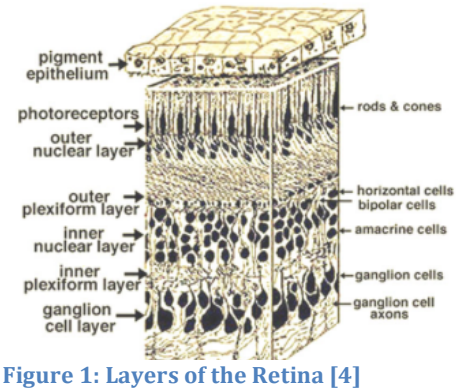

Figure 1: Layers of the Retina [4]

The Outer Nuclear Layer (ONL):

The ONL is composed of the rod and cone cell bodies. While cones are responsible for photopic, or color vision, rods are responsible for scotopic vision, or vision at low levels of light. When the photoreceptors react with light, they are hyperpolarized by the photons. This hyperpolarization results in a decreased release of glutamate, which directly affects the next, more anterior, layer of cell bodies, the INL. Between the ONL and the INL exists the OPL, which contains synaptic connections between the rods and cones and the cell bodies of the INL [1-3].

The Inner Nuclear Layer (INL):

The INL is composed of bipolar, horizontal, and amacrine cells. Bipolar cells directly synapse with both the cone and rod cell bodies and the ganglion cells of anterior portion of the retina. These cells function through a graded potential, as opposed to an all-or-nothing action potential. Therefore, the degree of glutamate released by the cones and rods affects the amount of glutamate released by the bipolar cells to the next cell bodies, the ganglion cells [1-3].

While the bipolar cells form direct connections, the horizontal and amacrine cells form lateral connections. Horizontal cells connect to one or more photoreceptors, which then conduct signals to bipolar cells that are innervated by other photoreceptors. Once depolarized by the photoreceptors, they release the inhibitory neurotransmitter, GABA, in a graded fashion to the bipolar cells at their terminal. This leads to a hyperpolarization of bipolar cells, and, therefore, results in a decreased release of glutamate [1-3].

The amacrine cells synapse with bipolar cells and conduct signals to ganglion cells that are innervated by other bipolar cells. Similar to horizontal cells, amacrine cells release GABA in a graded manner. This inhibitory neurotransmitter results in a hyperpolarization of the connected ganglion cell, and, thus, a lower probability that the cell will fire an action potential. Between the ganglion cell bodies and bipolar, horizontal, and amacrine cells exists a synaptic layer known as the IPL [1-3].

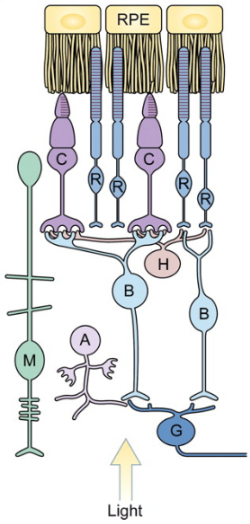

Figure 2: Depiction of Bipolar, Horizontal, and Amacrine Cells in Relation to the RPE and Photoreceptors [5]

The Ganglion Cell Layer (GCL):

The retina's complexity becomes even more apparent as the final output neurons are reached. Ganglion cells are not a one-size-fits-all type of neuron; rather, there are different types of these cells. Specifically, there are "ON" fibers and "OFF" fibers. While "ON" fibers are stimulated in the presence of light and inhibited in darkness, "OFF" fibers work contrary to that pattern. This leads to more precise signals that are eventually received by the brain [1-3].

The photoreceptors:

The photoreceptors line the back wall of the retina and are sensitive to the visible light portion of the electromagnetic spectrum, which lies between wavelengths 300nm and 850nm. Specifically, there are two types of photoreceptors, rods and cones. Rods are relatively sensitive compared to cones, as they are responsible for sensing photons in low light situations as well as sensing motion. Cones are able to sense color and bright light. On

average, the human retina contains approximately 3 million cones, which are generally centralized in the middle portion of the retina, termed the fovea centralis. Due to the high concentration of cones, the fovea is largely responsible for visual acuity. In contrast, there are roughly 100 million rods, which are dispersed throughout the periphery of this nervous system tissue [5].

The outer segments (OS) of the photoreceptors are responsible for the intake of photons. Moreover, rods contain stacks that are approximately 1000 disks tall and are densely concentrated with rhodopsin, a photoreceptive pigment. Rhodopsin is primarily comprised of two components, a colorless opsin protein, and a pigmented derivative of vitamin A, 11-*cis*-retinal. At rest, this molecule is in a *cis* configuration, but when rhodopsin absorbs light at approximately 500nm, 11-*cis*-retinal is isomerized to its all-*trans* form. Essentially, this isomerization results in phototransduction, which is a cascade of molecular events propagated by a G protein regulated module. This mechanism is responsible for the conversion of the physical light stimulus into an electrical signal. In times of darkness, the all-*trans*-retinal is isomerized back into 11-*cis*-retinal, which leads to a restoration of rhodopsin as well as the rod's sensitivity to dim light [5].

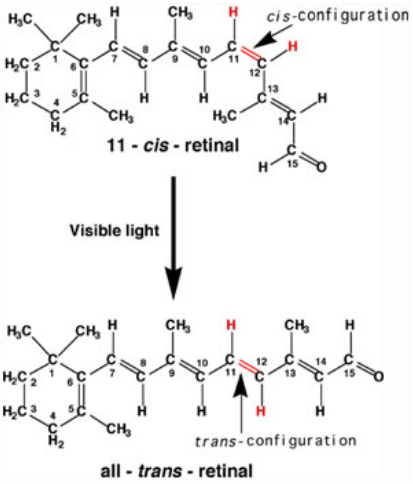

Figure 3 Conversion of 11-cis-retinal to all-trans-retinal [6]

Similar to rods, cones also contain visual pigments that are very comparable to rhodopsin. Rather than absorbing wavelengths at 500nm, there are three different types of cones that absorb light at three different wavelengths: blue light at 426nm, green light at

530nm, and red light at 560nm. A combination of these cone photoreceptors allows humans to observe all colors of the visual spectrum [5].

The Retinal Pigment Epithelium:

Light-detecting organs contain two types of cells, a photoreceptor cell that receives light as well as a pigmented cell. In humans, the light-absorbing pigmented cell type forms a layer that is referred to as the retinal pigment epithelium (RPE), which is located between the photoreceptor outer segments and the choroid. Both photoreceptor and pigmented cells are observed throughout all light-sensitive species in the animal kingdom, ranging from the simplest of insects to the more complex vertebrates [7]. Communication between the pigmented and photoreceptor cells is integral to visual function [8-11]. This trend is observed in genetic diseases of both types of cells. When there are mutated genes in photoreceptor cells, there is a primary RPE disorder and secondary retinal degeneration. Moreover, if there are mutations in the RPE, there are primarily problems in the retina, and secondarily problems in the RPE. Therefore, the interaction between the photoreceptors and RPE is integral to ocular health [8].

As previously stated, the RPE is composed of light-absorbing cells. These cells optimize vision by absorbing the scattered light that is not received by the photoreceptors. Because the RPE is pigmented, this was the most obvious function of this tissue, and, for a long time, light-absorption was believed to be the only purpose of the retinal pigment epithelium. However, the RPE has several other functions including: epithelial transport, spatial ion buffering, visual cycling, secretion, immune modulation, and phagocytosis [8].

The RPE is necessary for epithelial transport of blood from the choroid to the retina as well as from the sub-retinal space to the choroid. In order to facilitate this process, the RPE forms a tight-junction epithelial layer located between the choroid and the photoreceptors. These tight junctions form a blood/retina barrier that influences what is able to flow into and out of the retina. The main metabolites transported to the photoreceptors are glucose for energy metabolism, retinal for the visual cycle, and omega-fatty acids for formation of specialized phospholipids [12-14]. Water, ions, and metabolic waste are transported from the retina to the choroid and out of the eye [10, 15-18].

Ion buffering is another important task that is regulated by the RPE. This process is necessary due to the rapid ion changes within the sub-retinal space, which results from continual firing of the retina neurons [19]. Although there is a trans-epithelial mechanism for the transport of ions, this process is not rapid enough to keep the sub-retinal space in homeostasis. Therefore, the RPE provides other mechanisms that include voltage-dependent ion channels [20].

The visual cycle, as described in *The Photoreceptors* section, generates a buildup of all-*trans*-retinal in the photoreceptors [7,21]. Because the photoreceptors do not produce a re-isomerase enzyme, it is necessary for the all-*trans*-retinal to be transported to the RPE where it is re-isomerized to 11-*cis*-retinal. The 11-*cis*-retinal is then delivered back to the photoreceptors for future use [22-24].

Additionally, the RPE is able to interact with both the photoreceptors on its apical side and the choroid on its basolateral side by secreting a plethora of different growth factors. These growth factors function by preserving the structural integrity of the aforementioned adjacent structures [8]. Moreover, some growth factors function on a

continual basis, while others are only triggered if the RPE is strained, such as in times of hypoxia or metabolic stress. RPE secretion processes are mediated by Ca^{2+} dependent mechanisms [25-27].

The RPE also has immune system properties while still managing to protect the retina from the immunomolecules in the blood supply. This process is referred to as "immune privilege" and is accomplished in two ways: first, the tight junctions provide a blood/retina barrier that keep the immune system cells away, and, second, the RPE communicates with the immune system to silence immune activity when the retina is healthy, or to activate the immune system if the retina is diseased [28-30]. If necessary, the RPE secretes its own immunofactors to help heal an unhealthy retina [31-34].

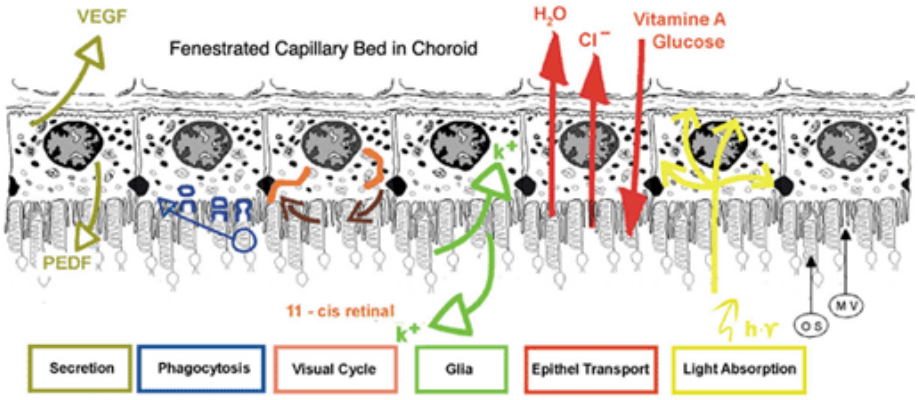

Figure 4: Overview of the major functions of the RPE [8]

Outer Segment Phagocytosis by the Retinal Pigment Epithelium:

The retinal pigment epithelium is also responsible for phagocytosis of the spent photoreceptor OS, which is the RPE function observed in this study. As previously mentioned, the cones and rods are continually damaged due to photo-oxidative stress. In order to maintain visual acuity, it is imperative that the damaged portions of the OS are

shed, identified, bound, ingested, and recycled by the RPE [9, 10, 35-39]. This process is diurnally mediated and is triggered by light [36-38, 40-43]. Interestingly, even nocturnal animals express a diurnal phagocytosis pattern [44]. Other than regulation by circadian rhythms, cone and rod maintenance is also controlled by communication between the RPE and photoreceptors. Specifically, there are three primary intermembrane receptors that have been identified to be involved in OS phagocytosis regulation: CD36, the receptor tyrosine kinase MERTK, and $\alpha_V\beta_5$ integrin. CD36 is responsible for internalization of the spent OS, $\alpha_V\beta_5$ integrin is required to bind to the OS, and MERTK activates the phagocytic mechanism [45-47]. The coordination between these proteins allows for regulation of effective OS phagocytosis.

$\alpha_V\beta_5$ integrin Mediated RPE Phagocytosis:

Outer segment binding requires the activation of $\alpha_V\beta_5$ integrin, an intermembrane protein lodged on the apical side of the RPE [48]. Moreover, $\alpha_V\beta_5$ integrin is responsible for sustaining contact between the RPE and photoreceptors [49], maintaining OS phagocytosis circadian rhythms [50], and also recognizing and binding to the spent OS by binding to its ligand, MFG-E8, on the integrin's extracellular domain. Rac1 then binds to $\alpha_V\beta_5$ on its cytoplasmic domain, resulting in the propagation of retinal phagocytosis [48, 50]. Subsequent activation of this protein results in phosphorylation and activation of focal adhesion kinase (FAK), further continuing the phagocytic mechanism by aiding in crosstalk between $\alpha_V\beta_5$ integrin and MERTK [51].

MERTK Mediated RPE Phagocytosis:

MERTK is part of the TAM (Tyro3, Axl, MERTK) family of receptor tyrosine kinases and is responsible for activation of the phagocytic mechanism [52]. While Tyro3 is also expressed in the RPE, previous studies have shown maintenance of OS phagocytosis in the absence of Tyro3 [53]. Conversely, OS phagocytosis ceases in the absence of MERTK, as seen in the Royal College of Surgeons (RCS) rat, which expresses a truncated and ineffective MERTK [54, 55]. Further studies identified retinal diseases associated with mutated human MERTK, such as retinitis pigmentosa. In both of these diseased models, lack of effective MERTK results in a loss of phagocytic uptake that results in a buildup of debris, which blocks transport of oxygen and nutrients to the retina. The eventual prognosis is atrophy of the retina, and, ultimately, blindness.

While MERTK is recognized as an integral component to OS phagocytosis, the mechanism involved is not completely understood. Current research shows that growth arrest-specific protein 6 (Gas6) and protein S (ProS) are ligands specific to TAM family proteins [52]. Also, communication between MERTK, $\alpha_V\beta_5$ integrin, and FAK result in the activation of MERTK by phosphorylation on specific tyrosine residues on MERTK [56]. These phosphotyrosine residues provide docking sites for Src-homology 2 (SH2) domain proteins, such as Grb2, P85α, Src, and Vav3

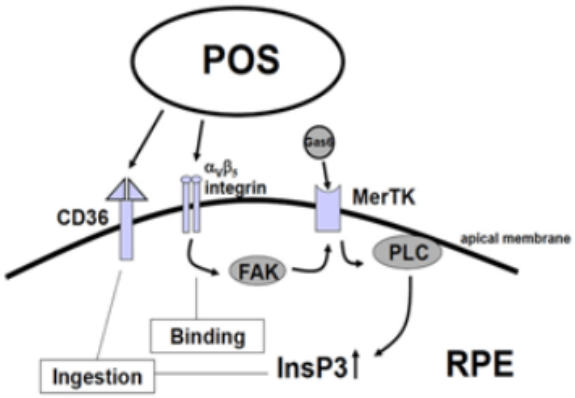

Figure 5: Molecules involved in the initiation of OS phagocytosis. Molecules discussed in thesis: POS- photoreceptor outer segments; CD36; $\alpha_V\beta_5$ integrin; FAK- focal adhesion kinase; MERTK- MER receptor tyrosine kinase; Gas6- growth arrest-specific protein 6 (could also be ProS- protein S) [8].

[57]. Generally, Grb2 and Vav3 play a role in cytoskeletal rearrangement [58-60], Src is involved in apoptotic cell clearance [59], and P85α contributes to downstream signaling processes that regulate inflammation [60, 61].

$\alpha_V\beta_5$ integrin and MERTK Dependent Actin and Myosin Redistribution:

Facilitation of spent OS ingestion is largely dependent on actin and myosin redistribution. Furthermore, it is known that $\alpha_V\beta_5$ integrin is the protein involved in actin rearrangement during RPE phagocytosis. After the initial binding of $\alpha_V\beta_5$ integrin to the OS, the integrin then activates Rac1. This alters actin arrangement, thus forming a phagocytic cup around the spent OS [62]. In RCS mice, actin rearrangement occurs, but phagocytosis is still inhibited, thus showing that MERTK is involved in the closure of the phagocytic cup, but not binding of the OS or formation of the cup [53]. MERTK executes this process by recruiting non-muscle myosin II to the ingestion site, thus engulfing the debris [63].

TAM Phagocytosis in Different Body Systems:

Other than the retina, the TAM (Tyro3, Axl, and Mertk) family group of transmembrane, tyrosine kinase proteins is largely responsible for phagocytic mechanisms in several body systems. Moreover, TAM family proteins are vital to the male reproductive system. Mice with a TAM triple knock-out (KO) mutation develop damaged Sertoli cells, resulting in degradation of most germ cells, such as spermatogonia, spermatocytes, and spermatids [64]. Under normal circumstances, the Sertoli cell is phagocytic and intakes apoptotic germ cells as well as other components of the germ cell [65, 66]. As more than half of the differentiating germ cells undergo apoptosis, phagocytosis of debris is critical

[66]. The consequences of toxic debris buildup due to ineffective Sertoli cells in TAM triple KO mice is similar to the loss of the phagocytic mechanism in the RPE; the former would ultimately become sterile, and the latter, blind [67].

There are several other TAM studies that have been conducted in many different body systems. These studies follow a similar methodology to the aforementioned Sertoli cell research in that they compare wild-type (WT) mice with intact TAM proteins to mice with single, double, and/or triple TAM KOs. For example, in the immune system, Mertk KO mice have slow-acting macrophages that are ineffective in clearing apoptotic cells (ACs) [68, 69]. This loss of phagocytosis is limited to the clearance of ACs, while the intake of yeast, bacteria, and silicone beads is still observed [70, 71]. The TAM family receptor tyrosine kinases also affects formation of red blood cells as a loss of MERTK in macrophages leads to a buildup of debris at erythroblastic islands [72]. Additionally, mammary glands accumulate a profound amount of ACs during lactation, resulting in the need for phagocytosis. In MERTK KO mice, these ACs were not phagocytized [73].

TAM family proteins also play a role in remodeling synapse space in the central nervous system, and, therefore, have implications in understanding of learning, memory, and neurological diseases [74]. Moreover, Tyro3 enhances the lifespan of neuropeptide Y, which helps regulate healthy feeding levels. Tyro3 mutant mice were found to exhibit behaviors associated with anorexia, which indicates that Tyro3 is potentially associated with feeding [75]. Up-regulation of Tyro3 was also found to lead to colorectal cancer, which indicates that normal expression of Tyro3 is necessary for colorectal health [76]. In general, deficiencies in TAM family proteins are associated with inflammatory and

autoimmune disorders, while elevated levels of TAM are linked to cancer, metastasis, and resistance to drug therapies [77].

New Research Implicating Tyro3's Importance in RPE Phagocytosis:

Previous research indicated the importance of MERTK as the sole TAM family tyrosine kinase responsible for RPE phagocytosis, but current studies show that Tyro3 may play a significant role in this phagocytic mechanism. Tyro3$^{-/-}$ mice were originally found to maintain intact retinas, and, therefore, some hypothesized that Tyro3 did not have an important role in OS phagocytosis, while others said that it was not necessary at all [53]. These theories came into question after observing that some humans experienced more slowly progressing retinal degeneration when compared to others. This is potentially due to the polymorphic nature of MERTK that results in different levels of protein expression and behavior. Furthermore, this trend was observed in RCS rats, which suggests that there is a genetic modifier responsible for the different levels of degeneration [79]. Eventually, Vollrath, et al. decided to run genetic studies to better understand Tyro3's importance in retinal phagocytosis [80].

During these studies, MERTK$^{-/-}$ mice were crossed for 10 generations in order to up-regulate Tyro3. Surprisingly, these mice had phenotypically normal retinas with areas of slight degeneration in the periphery. Overall, this research found that Tyro3 up-regulation can regulate photoreceptor degeneration, Tyro3 can promote OS phagocytosis, and that different levels of expression of both MERTK and Tyro3 can impact retinal phenotype [80].

Summation of Thesis:

Due to recent implications of Tyro3's importance in OS phagocytosis, the purpose of this research was to generate the tools necessary to test interactions between Tyro3 and SH2 domain proteins known to interact with MERTK. As Tyro3 and MERTK are familial receptor tyrosine kinases, it was hypothesized that they would exhibit similar interactions with SH2 domain proteins; however, research had not been conducted to study these interactions between Tyro3 and SH2 domain proteins in the RPE. First, using precisely designed primers, Tyro3 was truncated and inserted into pRSET A vector. Using bacterial constructs, these clones were then amplified and overexpressed to obtain the truncated protein. The protein was then purified for further interaction studies. The purified Tyro3 was subsequently used for pull-down assays to test interactions between the tyrosine kinase and SH2 domain proteins. These tests showed potential interactions between both Tyro3 and Vav1 and Tyro3 and Grb2, however, this data is still preliminary, and future studies will need to be conducted in order to confirm anything. These findings could be useful in understanding downstream interactions involved in OS phagocytosis. Understanding of this mechanism is integral in designing potential treatments for retinal diseases such as retinitis pigmentosa, and possibly even Age-Related Macular Degeneration. Previous gene therapies have been performed at the clinical level, but these studies were preliminary, and it is apparent that there is room for growth within this methodology [81]. The more that is known about the signaling mechanism behind RPE phagocytosis, the more effective future gene therapies will be.

Methods

Overview of Methods:

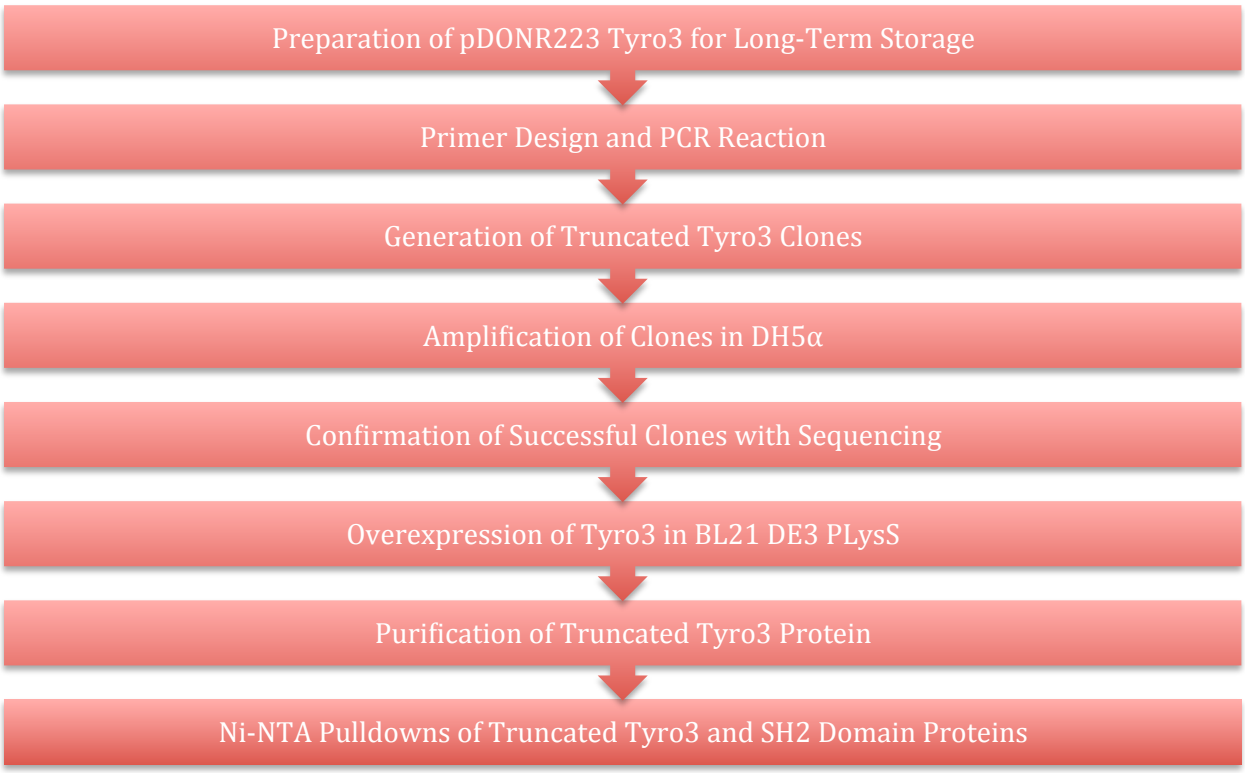

Preparation of pDONR223 Tyro3 for Long-Term Storage:

The pDONR223 Tryo3 vector was received in the form of a bacterial plug. This bacteria was then plated onto LB + Spectinomycin agar plates in order to select for pDONR223 Tyro3. Once grown, two colonies were selected, and both a large-scale overnight culture (50mL) and a small-scale overnight culture (5mL) were prepared. The following day, samples from each culture were used to prepare two glycerol stocks for long-term storage conditions at -80°C. The bacterial cultures were then centrifuged, and the pellet form the large-scale growth was used for extraction of DNA using a

ThermoScientific midi-prep kit. The pellet from the small-scale growth was used for extraction of DNA using an Invitrogen mini-prep kit.

Primer Design and PCR Reaction:

Tyro3 is an intermembrane protein, and, due to it containing both hydrophilic and hydrophobic portions, Tyro3 needed to be truncated in order to avoid solubility problems when testing for protein-protein interactions in-vitro. Therefore, primers were designed to truncate Tyro3 to include only the tyrosine kinase domain as well as the cytoplasmic tail. The primers were also designed to insert restriction enzyme cut sites (Xho1 and EcoR1) complementary to pRSET A, the vector that Tyro3 would eventually be cloned into. The pDONR223 Tyro3 template was run with the designed primers in a PCR reaction in order to amplify truncated Tyro3 DNA. The PCR reaction samples were run on gel electrophoresis to ensure successful cloning.

Generation of Truncated Tyro3 Clones:

Following the PCR reaction, the DNA samples were then cleaned using ThermoScientific GeneJET PCR Purification Kit. Next, both the truncated Tyro3 samples and the pRSET A vector were digested with Xho1 and EcoR1. The digested samples were then cleaned using the ThermoScientific kit. These samples were then ligated and transformed into DH5α cells for amplification and storage. Small-scale overnight growths were prepared by selecting colonies from the transformation plates. Glycerol stocks were then made from the overnight samples, and the rest of the sample was centrifuged. The DNA was then extracted from the bacterial pellets using the Invitrogen mini-prep kit.

Once extracted, a sample from each mini-prep was digested and run through gel electrophoresis for analysis of both insert and vector. The presence of two bands indicated that both insert and vector were present, while the presence of one band indicated that only vector was present. The potentially successful clones were then sent to MC Labs for sequencing, and the sequences were analyzed for mutations. The clones without mutations were chosen for subsequent studies.

Overexpression of the Tyro3 Truncations:

The non-mutated, truncated Tyro3 pRSET A clones were then transformed into BL21 DE3 PLysS cells for overexpression of Tyro3 DNA into protein using the *lac* operon. Small-scale (5mL) overnight growths were prepared from the transformation plate, and samples of each were taken for preparation of glycerol stocks. The overnights were additionally used to prepare large-scale (500mL) overexpression growths. The large-scale growths were incubated in a shaker to propagate bacterial growth. Protein production was then induced with IPTG, a derivative of lactose that cannot be hydrolyzed by lactase. If lactose were used in place of IPTG, the overexpression reaction would stop after sufficient levels of lactase were expressed; rather, IPTG is used and not hydrolyzed, thus leading to large-scale protein production. The overexpressions were centrifuged, the supernatant was removed, and the pellets were stored at -20^{o}C for future purification. Pre- and post-induction samples were taken and run on an SDS-PAGE gel to test for successful overexpression on an imager. The gel was then used for a western blot to assess for the appearance of protein using an antibody.

Purification of Truncated Tyro3 Protein:

The pellets from the overexpression reactions were mixed with lysis buffer (50mM Tris-HCl pH8, 200mM NaCl, 5% glycerol). The bacterial cells were then lysed using both lysozyme and sonication. In order to separate cellular components, ultra-centrifugation was run at a speed of 15,000rpm. The supernatant, which contained the truncated Tyro3 protein, was removed from the pellet and run through a Ni-NTA column to bind Tyro3. The column was washed twice with wash buffer (50mM Tris-HCl pH 8, 200mM NaCl, 5% glycerol, 25mM imidazole pH 8) to remove unbound protein, and Tyro3 was obtained in the three subsequent elutions using elution buffer (50mM Tris-HCl pH 8, 200mM NaCl, 5% glycerol, 250mM imidazole pH 8). The wash and elution samples were run on SDS-PAGE gels to ensure successful elution of truncated Tyro3 protein.

Ni-NTA Pulldowns of Truncated Tyro3 and SH2 Domain Proteins:

In order to determine protein concentration, Bradford assays were conducted on both the eluted Tyro3 protein and the GST-tagged SH2 domain proteins that were graciously provided by Dr. Shameka Shelby. These proteins were then used to conduct Ni-NTA pulldown assays to study potential interactions. The pulldown assays were performed by running two reactions, the first being the interaction study, and the second being the SH2 domain protein control group. The interaction study included incubation of Tyro3, the SH2 domain protein, and the Ni resin. The SH2 domain protein control group included the SH2 domain protein and the Ni resin. After incubation, the reactions were washed and the resulting protein was eluted. The interaction study, the SH2 domain control, the SH2

domain protein, and the Tyro3 protein were run on a SDS-PAGE gel to test for potential interactions.

Results

Primer Design and PCR Reaction:

As Tyro3 is a transmembrane protein, it contains both hydrophobic and hydrophilic regions. In order to avoid solubility problems when testing for interactions, the full-length Tyro3 protein needed to be truncated. Therefore, primers were designed to only generate Tyro3 DNA that included the tyrosine kinase domain and the cytoplasmic tail. The amino acids chosen for truncation were 470, 490, and 498. These locations were chosen after studying the human Tyro3 sequence on ncbi. Following this analysis, primers were designed to truncate in these regions during PCR amplification. The PCR reaction was successful for reactions 470 and 498 as seen by the large concentration of DNA that migrated to approximately 1,200 base pairs, which was the expected number of base pairs (Figure 6). The 490-truncation reaction did not generate a large concentration of DNA, and further PCR reactions were not very successful. Additionally, the full-length Tyro3 was not generated in this reaction, but future reactions were able to amplify full-length DNA for future mammalian construct interaction studies.

Generation of Truncated Tyro3 Clones:

After digestion, ligation, and further amplification (Figure 7) of the Tyro3 + pRSET A reactions, samples were digested and run on gel electrophoresis to assess for the presence of two bands, one representing insert, and the other representing vector. The gel indicated the presence of both vector and insert for several samples. The vector bands were located under the 3,000bp mark, and the insert bands were located at approximately 1,200bp. The bands located under 6,000bp indicate the presence of uncut DNA (Figure 8).

Overexpression and Purification of Truncated Tyro3:

Following the overexpression and purification of Tyro3, the washes and elutions from the purification step were run on SDS-PAGE gel to ensure that Tyro3 was successfully obtained (Figures 9 & 10). Figure 9 shows the elution of two 470-truncation proteins, and Figure 10 shows the elution of two 498-truncation proteins. The eluted single Tyro3 protein migrated to approximately 33kD, which was expected; however, Tyro3, and tyrosine kinases in general, are known to dimerize. Therefore the Tyro3 dimer was also eluted, as seen by the bands at approximately 66kD.

Ni-NTA Pulldowns of Truncated Tyro3 and SH2 Domain Proteins:

Preliminary pulldown assays were conducted to assess potential interactions between Tyro3 and SH2 domain proteins (Figure 11 & 12). For each pulldown assay, four lanes were loaded into the SDS-PAGE gel. The first lane contained the SH2 domain protein, the second contained the SH2 domain protein and Ni resin control, the third contained the Ni-NTA pulldown assay interaction study between Tyro3 and the SH2 domain protein, and the fourth lane contained Tyro3. All four pulldown assays indicated the presence of both Tyro3 and the SH2 domain protein; however, Vav2 and Vav3 showed similar concentrations for SH2 domain protein in both the control lane and the interaction study lane. This shows that the Vav2 and Vav3 potentially interacted with the Ni resin better than with Tyro3. Nevertheless, Vav1 (Figure 11) and Grb2 (Figure 12) bands in the interaction lanes are more concentrated than in the control lanes, which indicates that Vav1 and Grb2 may interact with Tyro3.

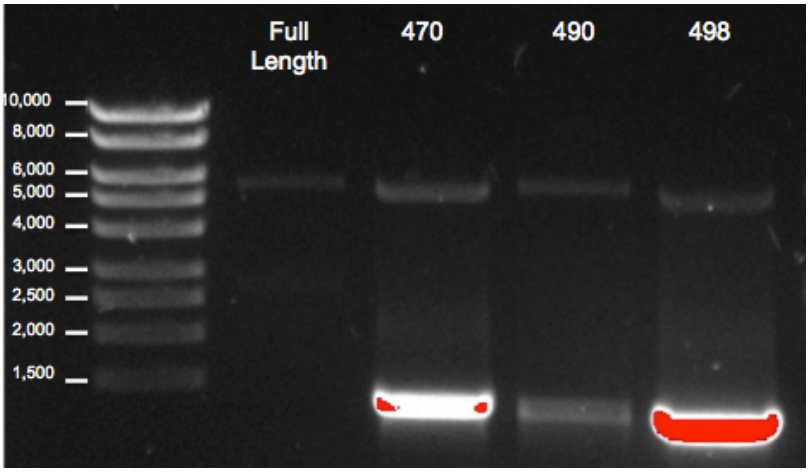

Figure 6: visualization of Tyro3 truncation PCR reactions. Specialized primers were utilized to truncate Tyro3 at the indicated sites (470 & 498).

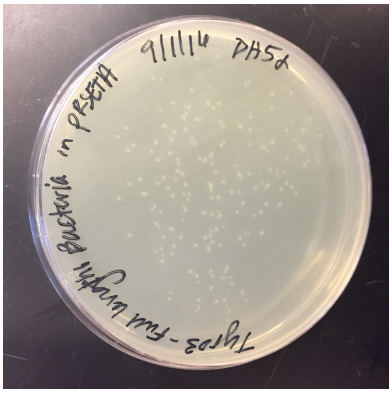

Figure 7: transformation into DH5α for amplification and storage.

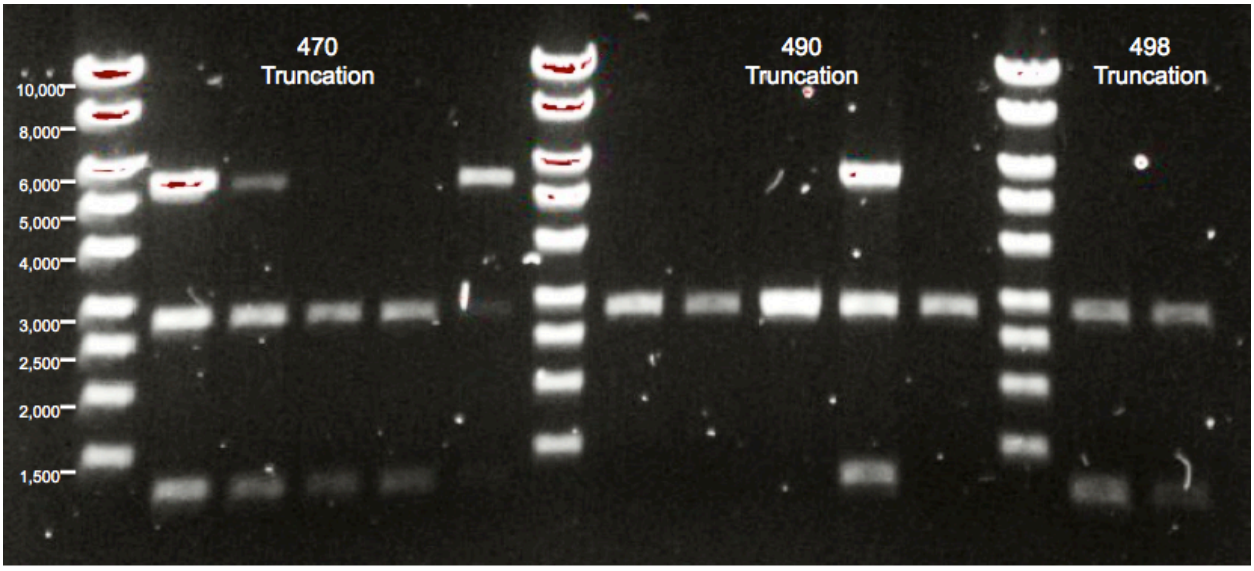

Figure 8: Insert and Vector. The appearance of two bands on the SDS-PAGE gel indicates that the truncated Tyro3 DNA was inserted into the vector.

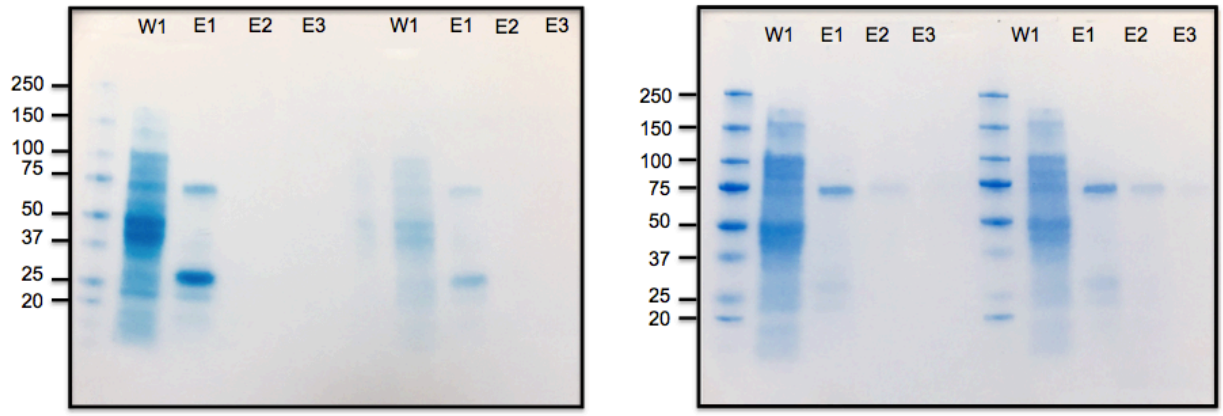

Figures 9 & 10: Tyro3 470 (left) and 498 (right) truncation purifications. A 6xHis-tag that was engineered into the pRSET A vector was able to interact with the Ni-NTA column. The column was washed two times and the truncated Tyro3 was then eluted. Labels: W1- Wash 1; W2- Wash 2; E1- Elution 1; E2- Elution 2; E3- Elution 3.

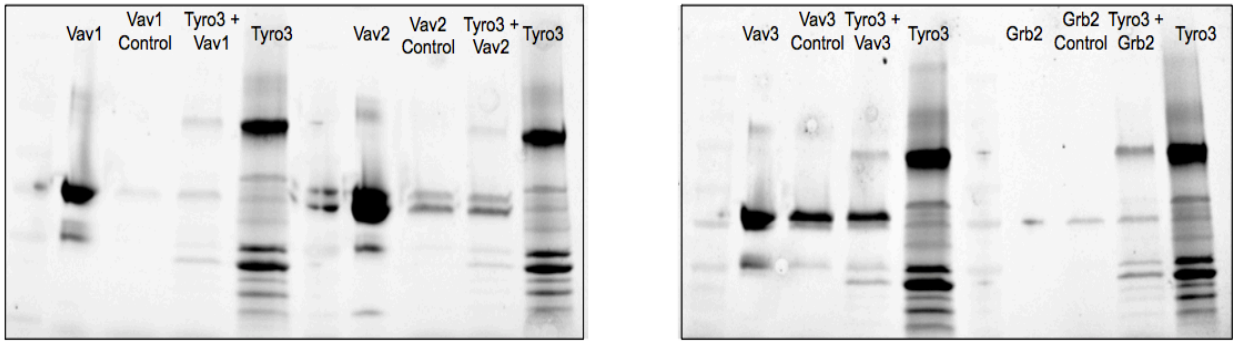

Figures 11 & 12: Preliminary Ni-NTA pulldown assays. Ni-NTA pulldown assayswere conducted in order to asess potential interactions between Tyro3 and the SH2 domain proteins: Vav1, Vav2, Vav3, and Grb2.

Discussion and Conclusion

Tyro3 was successfully truncated at amino acid 470 and at amino acid 498 using PCR amplification, but the 490-truncation reaction was never prosperous as only low concentrations of this reaction were continually generated (Figure 6). This could be due to improper primer design, primer hairpins, or a lack of affinity of the primer for the DNA. A different 490-truncation primer could have been designed to try to resolve these potential problems, however, because the 470- and 498-truncations were successful, 490-truncation primers were never re-designed.

After further amplification of the DNA (Figure 7), the truncated Tyro3 was successfully cloned into pRSET A vector by using restriction enzyme digestion of both the vector and the insert and subsequent ligation of these two components together. The cloning reactions were found to be successful after observation of both insert and vector using gel electrophoresis analysis (Figure 8). The 470- and 498-truncation reactions resulted multiple potential clones, but the 490-truncation only resulted one. Further sequencing was used to select the samples without mutations, which, once more, indicated the success of the 470- and 498-truncations, and the failure of the 490-trancation. This was likely due to the low concentration of the 490-truncation DNA originally generated in the previous PCR amplification reaction. If more had been generated, it is probable that there would have been more successful clones and a higher chance that at least one of the clones would not have exhibited mutations. Regardless, the 470- and 498-truncations were chosen for future studies.

Using the *lac* operon, the chosen DNA clones were then overexpressed in bacterial constructs in order to generate truncated Tyro3 protein. The protein was then successfully purified using Ni-NTA, which was able to interact with the 6x His tag that was engineered into the N-terminus of the protein from the pRSET A vector (Figures 9 & 10). Although truncated Tyro3 was purified, its dimer was eluted as well. In order to achieve the correct Tyro3 and SH2 domain protein ratios during protein interaction studies, the Tyro3 dimer is not desirable. Future studies will troubleshoot BME concentrations in order to fully denature disulfide bonds. These studies will also find the necessary salt concentrations to prevent the electrostatic interactions that result in the dimer.

The purified 470-truncation was then chosen to run preliminary Ni-NTA pulldown assay interaction studies (Figures 11 & 12). During these studies, Tyro3 and chosen SH2 domain proteins were incubated with Ni resin, which is known to interact with the 6x His tag that was engineered onto the N-terminus of the protein. Subsequent washes removed the SH2 domain protein if not bound to Tyro3. The Tyro3 was then eluted, and if Tyro3 had interacted with the SH2 domain protein, two bands would be observed when the samples were run on an SDS-PAGE gel, one indicating the presence of Tyro3, and the other indicating the presence of the SH2 domain protein. A Ni resin and SH2 domain protein control sample was also incubated, washed, and eluted to test for potential interaction between the Ni resin and the SH2 domain protein.

The pulldown assay, SH2 domain protein control, SH2 domain protein, and Tyro3 were then run on an SDS-PAGE gel for analysis of interaction. When examining the gel, the first discovery was that Tyro3 was not purified as well as it could have been. Size exclusion chromatography will be utilized in the future for better purification. Moreover, the

presence of both Tyro3 and SH2 domain protein was found in all four pulldown assays, but the Vav2 and Vav3 studies showed comparable concentrations of SH2 domain protein in both the control group and the pulldown assay group, which indicates that Vav2 and Vav3 probably interacted better with the Ni resin than with Tyro3. However, Vav1 and Grb2 showed higher concentrations of SH2 domain protein in the pulldown group than in the control group, which indicates potential protein-protein interactions. Nevertheless, these studies are still preliminary, and more pulldown assays will need to be conducted before any interactions are confirmed.

Future Research

Future research will include more pulldown assays to identify interactions between Tyro3 and SH2 domain proteins in bacterial constructs. Once these interactions are detected, this research will begin to move in a more in-vivo direction. Full-length Tyro3, which was previously cloned into pcDNA 3.1 His vector, will be transfected into cell culture, and Tyro3 will be overexpressed. Tyro3 protein-protein interactions will then be assessed using co-immunoprecipitation reactions. The interactions found in mammalian constructs will then be compared to the interactions found in bacterial constructs.

After confirmation of in-vitro interactions in both bacterial and mammalian constructs, these interactions will be further assessed by determination of the specific phosphotyrosine residues that the SH2 domain proteins interact with. These studies will be conducted by facilitating a tyrosine to phenylalanine mutation of the truncated Tyro3 by using primers designed for site-directed mutagenesis. The truncated Tyro3 mutant will then be overexpressed, purified, and used for pulldown assay interaction studies. If a loss of interaction is observed, the mutated tyrosine residue will be noted as a docking site for the studied SH2 domain protein.

Further directions will confirm these protein-protein interactions using in-vivo studies. Both wild type and Tyro3 KO mice will be obtained and their retinas will be carefully extracted and lysed to use for western blot and flow cytometry immuno-studies. The interactions found in these methods will then be compared to those found in the in-vitro bacterial and mammalian constructs conducted prior.

Acknowledgements

I would like to thank Dr. Shelby for her immense knowledge and guidance throughout the research process. I would also like the thank the Florida Southern College Chemistry and Biology Departments for the resources necessary to conduct this research, as well as the Honors Program for the opportunity to compose this thesis.

References

1. Polyak, S.L., *The Retina*1941, Chicago: University of Chicago.
2. Kolb, H., *The neural organization of the human retina.*, in *Principles and practice of clinical electrophysiology of vision*, J.R. Heckenlively and G.B. Arden, Editors. 1991, Mosby Year Book: St. Louis. p. 25-52.
3. Van Buren, J.M., *The retinal ganglion cell layer : a physiological-anatomical correlation in man and primates of the normal topographical anatomy of the retinal ganglion cell layer and its alterations with lesions of the visual pathways*1963, Springfield, Ill.: Charles C. Thomas. x, 143 p.
4. Kolb, H., Fernandez, E., Nelson, R. (2012) Simple Anatomy of the Retina. Salt Lake City Utah: University of Utah Heath Sciences Center.
5. Sung, C.H., Chuang, J.Z. (2010) The Cell Biology of Vision. J Cell Biol 190 (6): 953.
6. Casiday, R., Frey, R. Vision and Light-Induced Molecular Changes: Spectroscopy and Quantum Chemistry Experiment. Department of Chemistry, Washington University.
7. Lamb, T.D., Colling, S.P., Pugh, E.N., Jr. (2007) Evolution of the vertebrate eye: opsins, photoreceptors, retina and eye cup. Nat Rev Neurosci 8:960-976.
8. Strauss, O. (2005) The retinal pigment epithelium in visual function. Physiol Rev 85:845-881.
9. Bok, D. (1993) The retinal pigment epithelium: a versatile partner in vision. J Cell Suppl 17:189-195.
10. Steinberg, R.H. (1985) Interactions between the retinal pigment epithelium and the neural retina. Doc Ophthalmol 60:327-346.
11. Sparrow, J.R., Hicks, D., Hamel, C.P. (2010) The retinal pigment epithelium in health and disease. Curr Mol Med 10:802-823.
12. Ban, Y., Rizzolo, L.J. (2000) Regulation of glucose transporters during development of the retinal pigment epithelium. Brain Res Dev Brain Res 121:89-95.
13. Bazan, N.G., Gordon, W.C., Rodriguez de Turco, E.B. (1992) Docosahexaenoic acid uptake and metabolism in photoreceptors: retinal conservation by an efficient retinal pigment epithelial cell-mediated recycling process. Neurobiology of Essential Fatty Acids:295-306.
14. Bazan, N.G., Rodriguez de Turco, E.B., Gordon, W.C., (1994) Docosahexaenoic acid supply to the retina and its conservation in photoreceptor cells by active retinal pigment epithelium-mediated recycling. World Rev Nutr Diet 75:120-123.
15. Miller, S.S., Steinberg, R.H. (1977) Active transport of ions across frog retinal pigment epithelium. Exp Eye Res 25:235-248.
16. Miller, S.S., Steinberg, R.H. (1977) Passive ionic properties of frog retinal pigment epithelium. J Membr Biol 36:337-372.
17. Hughes, B.A., Gallemore, R.P., Miller, S.S. (1998) Transport mechanisms in the retinal pigment epithelium. In: Marmor, M.F., Wolfensberger, T.J. (eds) The retinal pigment epithelium. Oxford University Press, New York, Oxford, pp. 103-134.
18. Hamann, S. (2002) Molecular mechanisms of water transport in the eye. Int Rev Cytol 215:395-431.
19. Steinberg, R.H., Linsenmeier, R.A., Griff, E.R. (1983) Three light-evoked responses of the retinal pigment epithelium. Vision Res 23:1315-1323.
20. Baylor, D. (1996) How photons start vision. Proc Natl Acad Sci USA 93:560-565.

21. Lamb, T.D., Pugh, E.N., Jr. (2004) Dark adaption and the retinoid cycle of vision. Prog Retin Eye Res 23:307-380.
22. Baehr, W., Wu, S.M., Bird, A.C., Palczewski, K. (2003) The retinoid cycle and retina disease. Vis Res 43:2957-2958.
23. Thompson, D.A., Gal, A. (2003) Vitamin A metabolism in the retinal pigment epithelium: genes, mutations, and diseases. Prog Retin Eye Res 22:683-703.
24. Thompson, D.A., Gal, A. (2003) Genetic defects in vitamin A metabolism of the retinal pigment epithelium. Dev Ophthalmol 37:141-154.
25. Rosenthal, R., Strauss, O. (2002) Ca^{2+} -channels in the RPE. Adv Exp Med Biol 514:225-235.
26. Catterall, W.A. (2000) Structure and regulation of votage-gated Ca^{2+} channels. Annu Rev Cell Dev Biol 16:521-555.
27. Striessnig, J. (1999) Pharmacology, structure and function of cardiac L-type Ca^{2+} channels. Cell Physiol Biochem 9:242-269.
28. Ishida, K., Panjwani, N., Cao, Z., Streilein, J.W., (2003) Participation of pigment epithelium in ocular immune privilege. 3. Epithelia cultured from iris, ciliary body, and retina suppress T-cell activation by partially non-overlapping mechanisms. Ocul Immunol Inflamm 11:91-105.
29. Streilein, J.W., Ma, N., Wenkel, H., Ng, T.F., Zamiri, P. (2002) Immunobiology and privilege of neuronal retina and pigment epithelium transplants. Vision Res 42:487-495.
30. Wenkel, H., Streilein, J.W. (2000) Evidence that retinal pigment epithelium functions as an immune-privileged tissue. Ivest Ophthalmol Vis Sci 41:3467-3473.
31. Relvas, L.J., Bouffioux, C., Marcet, B., Communi, D., Makhoul, M., Horckmans, M., Blero, D., Bruyns, C., Caspers, L., Boeynaems, J.M., Willermain, F. (2009) Extracellular nucleotides and interleukin-8 production by ARPE cells: potential role of danger signals in blood-retinal barrier activation. Invest Ophthalmol Vis Sci 50:1241-1246.
32. Kim, Y.H., He, S., Kase, S., Kitamura, M., Ryan, S.J., Hinton, D.R. (2009) Regulated secretion of complement factor H by RPE and its role in RPE migration. Graefes Arch Clin Exp Ophthalmol 247:651-659.
33. Chen, M., Forrester, J.V., Xu, H. (2007) Synthesis of complement factor H by retinal pigment epithelial cells is down-regulated by oxidized photoreceptor outer segments. Exp Eye Res 84:635-645.
34. Austin, B.A., Liu, B., Li, Z., Nussenblatt, R.B. (2009) Biologically active fibronectin fragments stimulate release of MCP-1 and catabolic cytokines from murine retinal pigment epithelium. Invest Ophthalmol Vis Sci 50:2896-2902.
35. Strauss, O., Stumpff, F., Mergler, S., Wienrich, M. (1998) The Royal College of Surgeons Rat: an animal model for inherited retinal degeneration with a still unknown genetic defect. Acta Anat (Basel) 162: 101-111.
36. LaVail, M.M. (1976) Rod outer segment disc shedding in relation to cyclic lighting. Exp Eye Res 23:277-280.
37. LaVail, M.M. (1980) Circadian nature of rod outer segment disc shedding in the rat. Invest Opthalmol Vis Sci 19:407-411.
38. LaVail, M.M. (1983) Outer segment disc shedding and phagocytosis in the outer retina. Trans Ophthalmol Soc U K 103 (Pt 4): 397-404.

39. Kevany, B.M., Palczewski, K. (2010) Phagocytosis of retinal rod and cone photoreceptors. Physiology (Bethesda) 25: 8-15.
40. Green, C.B., Besharse, J.C. (2004) Retinal circadian clocks and control of retinal physiology. J Biol Rhythms 19:91-102.
41. Besharse, J.C., Defoe, D.M. (1998) Role of the retinal pigment epithelium in photoreceptor membrane turnover. In: Marmor, M.F., Wolfensberger, T.J. (eds) The retinal pigment epithelium. Oxford University Press, Oxford, pp. 152-172
42. Besharse, J.C., Hollyfield, J.G. (1979) Turnover of mouse photoreceptor outer segments in constant light and darkness. Invest Ophthalmol Vis Sci 18:1019-1024.
43. Beharse, J.C., Hollyfield, J.G., Rayborn, M.E. (1977) Photoreceptor outer segments: accelerated membrane renewal in rods after exposure to light. Science 196:536-538.
44. Bobu, C. Hicks, D. (2009) Regulation of retinal photoreceptor phagocytosis in a diurnal mammal by circadian clocks and ambient lighting. Invest Ophthalmol Vis Sci 50:3495-3502.
45. Finnemann, S.C., Silverstein, R.L. (2001) Differential roles of CD36 and alphavbeta5 integrin in photoreceptor phagocytosis by the retinal pigment epithelium. J Exp Med 194: 1289-1298.
46. Finnemann, S.C., et al. (1997) Phagocytosis of rod outer segments by retinal pigment epithelial cells requires alpha(v)beta5 integrin for binding but not for internalization. Proc Natl Acad Sci U S A 94(24): p. 12932-7.
47. Nandrot, E.F., et al. (2006) Novel role for alphavbeta5-integrin in retinal adhesion and its diurnal peak. Am J Physiol Cell Physiol. 290(4): p. C1256- 62.
48. Nandrot, E.F. and S.C. Finnemann (2006) Altered rhythm of photoreceptor outer segment phagocytosis in beta5 integrin knockout mice. Adv Exp Med Biol, 572: p. 119-23.
49. Finnemann, S.C. (2003) Focal adhesion kinase signaling promotes phagocytosis of integrin-bound photoreceptors. Embo J. 22(16): p. 4143-54.
50. Nandrot, E.F., et al. (2004) Loss of synchronized retinal phagocytosis and age-related blindness in mice lacking alphavbeta5 integrin. J Exp Med. 200(12): p. 1539-45.
51. Stitt TN, Conn G, Gore M, Lai C, Bruno J, et al. (1995) The anticoagulation factor protein S and its relative, Gas6, are ligands for the Tyro 3/Axl family of receptor tyrosine kinases. Cell 80: 661–670.
52. D'Cruz PM, Yasumura D, Weir J, Matthes MT, Abderrahim H, et al. (2000) Mutation of the receptor tyrosine kinase gene Mertk in the retinal dystrophic RCS rat. Hum Mol Genet 9: 645–651.
53. Feng W, Yasumura D, Matthes MT, LaVail MM, Vollrath D (2002) Mertk triggers uptake of photoreceptor outer segments during phagocytosis by cultured retinal pigment epithelial cells. J Biol Chem 277: 17016–17022.
54. Wu Y, Singh S, Georgescu MM, Birge RB (2005) A role for Mer tyrosine kinase in alphavbeta5 integrin-mediated phagocytosis of apoptotic cells. J Cell Sci 118: 539–553.
55. Shelby, S.J., Colwill, K., Dhe-Paganon, S., Pawson, T., & Thompson, D.A. (2013) MERTK Interactions with SH2-Domain Proteins in the Retinal Pigment Epithelium. PLoS ONE

56. Tibrewal N, Wu Y, D'Mello V, Akakura R, George TC, et al. (2008) Autophosphorylation docking site Tyr-867 in Mer receptor tyrosine kinase allows for dissociation of multiple signaling pathways for phagocytosis of apoptotic cells and down-modulation of lipopolysaccharide-inducible NF-kappaB transcriptional activation. J Biol Chem 283: 3618–3627.
57. Giubellino A, Burke TR Jr, Bottaro DP (2008) Grb2 signaling in cell motility and cancer. Expert Opin Ther Targets 12: 1021–1033.
58. Bustelo XR (2000) Regulatory and signaling properties of the Vav family. Mol Cell Biol 20: 1461–1477.
59. Yi Z, Li L, Matsushima GK, Earp HS, Wang B, et al. (2009) A novel role for c-Src and STAT3 in apoptotic cell-mediated MerTK-dependent immunoregulation of dendritic cells. Blood 114: 3191–3198.
60. Zoncu R, Efeyan A, Sabatini DM (2011) mTOR: from growth signal integration to cancer, diabetes and ageing. Nat Rev Mol Cell Biol 12: 21–35.
61. Simonsen A, Lippe R, Christoforidis S, Gaullier JM, Brech A, et al. (1998) EEA1 links PI(3)K function to Rab5 regulation of endosome fusion. Nature 394: 494–498.
62. Mao, Y., & Finnemann, S.C. (2012). Essential diurnal Rac 1 activation during retinal phagocytosis requires $\alpha_V\beta_5$ integrin but not tyrosine kinases focal adhesion kinase or Mer tyrosine kinase. Molecular Biology of the Cell, 23(6), 1104-1114.
63. Strick, D.J., Feng, W., Vollrath, D. (2009) Mertk drives myosin II redistribution during retinal pigment epithelial phagocytosis. Invest Ophthalmol Vis Sci 50: 2427-2435
64. Lu, Q. Gore, M., Zhang, Q. Camenisch, T., Boast, S., Casagranda, F., Lai, C., Skinner, M.K., Klein, R., Matsushima, G.K., Earp, H.S., Goff, S.P., Lemke, G., 1999. Tyro-3 family receptors are essential regulators of mammalian spermatogenesis. Nature 398, 723-728.
65. Kerr, J.B., Mayberry, R.A., Irby, D.C., 1984. Morphometric studies on lipid inclusions in Sertoli cells during the spermatogenic cycle in the rat. Cell Tissue Res. 236, 699-709.
66. Nakanishi, Y., Shiratsuchi, A., 2004. Phagocytic removal of apoptotic spermatogenic cells by Sertoli cells: mechanisms and consequences. Biol. Pharm. Bull. 27, 13-16.
67. Prasad, D., Rothlin, C.V., Burrola, P., Burstyn-Cohen, T., Lu, Q., de Frutos, P.G., Lemke, G., 2006. TAM receptor function in the retinal pigment epithelium. Mol. Cell. Neurosci. 33, 96-108.
68. Scott, R.S., McMahon, E.J., Pop, S.M., Reap, E.A., Caricchio, R., Cohen, P.L., Earp, H.S., Matsushima, G.K., 2001. Phagocytosis and clearance of apoptotic cells in mandated by MER. Nature 411, 207-211.
69. Cohen, P.L., Caricchio, R., Abraham, V., Camenisch, T.D., Jennette, J.C., Roubey, T.A., Earp, H.S., Matsushima, G., Reap, E.A., 2002. Delayed apoptotic cell clearance and lupus-like autoimmunity in mice lacking the c-mer membrane tyrosine kinase. J. Exp. Med. 196, 135-140.
70. Lu, Q., Lemke, G., 2001. Homeostatic regulation of the immune system by receptor tyrosine kinases of the Tyro 3 family. Science 293, 306-311.
71. Lemke, G., Lu, Q., 2003. Macrophage regulation by Tyro 3 family receptors. Curr. Opin. Immunol. 15, 31-36.
72. Toda S, Segawa K, Nagata S (2014) MerTK-mediated engulfment of pyrenocytes by central macrophages in erythroblastic islands. Blood 123: 3963–3971.

73. Sandahl M, Hunter DM, Strunk KE, Earp HS, Cook RS (2010) Epithelial cell-directed efferocytosis in the post-partum mammary gland is necessary for tissue homeostasis and future lactation. BMC Dev Biol 10: 122
74. Chung WS, Clarke LE, Wang GX, Stafford BK, Sher A, et al. (2013) Astrocytes mediate synapse elimination through MEGF10 and MERTK pathways. Nature 504: 394–400.
75. Kim, D.Y., Yu, J., Mui, R.K., Niibori, R., Taufique, H.B., Aslam, R., Semple, J.W., Cordes, S.P. (2017) The tyrosine kinase receptor Tyro3 enhances lifespan and neuropeptide Y (Npy) neuron survival in the mouse anorexia (anx) mutation. Dis Model Mech. Doi: 10.1242
76. Schmitz, R., Valls, A.F., Yerbes, R., Von Richter, S., Kahlert, C., Loges, S., Weitz, J., Schneider, M., Ruiz de Almodovar, C., Ulrich, A., Schmidt, T. (2016) TAM receptor Tyro3 and Mer as novel targets in colorectal cancer. Oncotarget 7: 56355-56370.
77. Lemke G (2013) Biology of the TAM Receptors. Cold Spring Harb Perspect Biol 5.
78. Seitz HM, Camenisch TD, Lemke G, Earp HS, Matsushima GK (2007) Macrophages and dendritic cells use different Axl/Mertk/Tyro3 receptors in clearance of apoptotic cells. J Immunol 178: 5635-5642. PMID: 17442946
79. Tschernutter M, Jenkins SA, Waseem NH, Saihan Z, Holder GE, et al. (2006) Clinical characterization of a family with retinal dystrophy caused by mutation of Mertk gene. Br J Ophthalmol 90: 718-723. PMID: 16714263
80. Vollrath D, Yasumura D, Benchorin G, Matthes MT, Feng W, Nguyen NM, Sedano CD, Calton MA, LaVail MM (2015) *Tyro3* Modulates *Mertk*-Associated Retinal Degeneration. Plos Genetics
81. Ghazi, N.G., Abboud, E.B., Nowilaty, S.R., Alkuraya, H., Alhommadi, A., Cai, H., Hou, R., Deng, W.T., Boye, S.L., Almaghamsi, A., Al Saikhan, F., Al-Dhibi, H., Birch, D., Chung, C., Cloak, D., LaVail, M.M., Vollrath, D., Erger, K., Wang, W., Conlon, T., Zhang, K., Hauswirth, W., Alkuraya, F.S. (2016) Treatment of retinitis pigmentosa due to MERTK mutations by ocular subretinal injection of adeno-associated virus gene vector: results of a phase I trial. Hum Genet 135: 327-343.